MINIMIZING EMITTANCE FOR THE CLIC DAMPING RING

E. Levitchev, P. Piminov, S. Siniatkin, P. Vobly, K. Zolotarev, BINP
H.H. Braun, M. Korostelev, D. Schulte, F. Zimmermann, CERN

Abstract

The CLIC damping rings aim at unprecedented small normalized equilibrium emittances of 3.3 nm vertical and 550 nm horizontal, for a bunch charge of $2.6\cdot10^9$ particles and an energy of 2.4 GeV. In this parameter regime the dominant emittance growth mechanism is intra-beam scattering. Intense synchrotron radiation damping from wigglers is required to counteract its effect.

Here the overall optimization of the wiggler parameters is described, taking into account state-of-the-art wiggler technologies, wiggler effects on dynamic aperture, and problems of wiggler radiation absorption. Two technical solutions, one based on superconducting magnet technology the other on permanent magnets are presented.

Although dynamic aperture and tolerances of this ring design remain challenging, benefits are obtained from the strong damping. For optimized wigglers, only bunches for a single machine pulse may need to be stored, making injection/extraction particularly simple and limiting the synchrotron-radiation power. With a 365 m circumference the ring remains comparatively small.

INTRODUCTION

The design of the CLIC damping ring is based on a racetrack shape with the two 180^0 arcs made from 48 TME cells each and long straight sections to accommodate long damping wigglers. The circumference of the ring is 365 m with a total wiggler length of 152 m. The beam energy is 2.42 GeV. More information can be found in [1-5].

At zero beam current the equilibrium emittance of the arcs is well below the design goals of 3.3 nm vertical, 550 nm horizontal and 5 keVm longitudinal (r.m.s., normalized). For the nominal bunch charge of $2.6\cdot10^9$ particles, however, intra beam scattering (IBS) becomes a major source of emittance growth, requiring balancing with strong damping from the wigglers.

Therefore a strong wiggler on axis peak field B_w is desirable with damping from the wigglers increasing like B_w^2. The contribution from the wigglers to the synchrotron radiation induced part of the equilibrium emittance, however, increases like $B_w^3\lambda_w^2$, and approximately the same scaling applies to the contribution from IBS. Therefore, an increase of B_w has to be associated with a decrease of the wiggler period at least in proportion like $\lambda_w \sim B_w^{-3/2}$. A more detailed analytical treatment of the interdependence between emittance wiggler field and wiggler period in the presence of synchrotron radiation and IBS can be found in [6].

In this paper we describe the calculation of optimum wiggler parameters in the presence of IBS and we show two technical solutions for the wigglers. The first one is based on permanent magnet technology the second on a superconducting wiggler design. The related problem of evacuation of the heat generated by the wiggler radiation is treated in a recently published CLIC note [7]. In this context it is interesting to mention that the average synchrotron radiation power does not necessarily increase with an increase of B_W. Since the damping time decrease in proportion with the power radiated per electron the required minimum storage time for damping from injection to extraction emittance is reduced. Therefore the total radiated power is only a function of the damping ring energy, the mean current extracted and the ratio of injected emittance to extracted emittance.

CHOICE OF PARAMETERS

Using the modified Piwinski formalism the equilibrium transverse emittances $\gamma\varepsilon_x$, $\gamma\varepsilon_y$ in the presence of IBS are computed as a function of the wiggler peak field B_w and period length λ_w in the range $1.7\ \mathrm{T}<B_w<2.9\ \mathrm{T}$ and $1\ \mathrm{cm}<\lambda_w<11\ \mathrm{cm}$, respectively. The simulations were done for a bunch population of $N_B=2.56\cdot10^9$ and a betatron coupling of 0.63%. The RF voltage for each B_w, λ_w combination was adjusted to keep the equilibrium longitudinal emittance at $\gamma\varepsilon_L=5000$ eV·m. The results of this scan is shown in Fig. 1 . As can be seen from Fig. 1, at a fixed value of wiggler period λ_w the horizontal emittance is minimized for an optimum value of B_w.

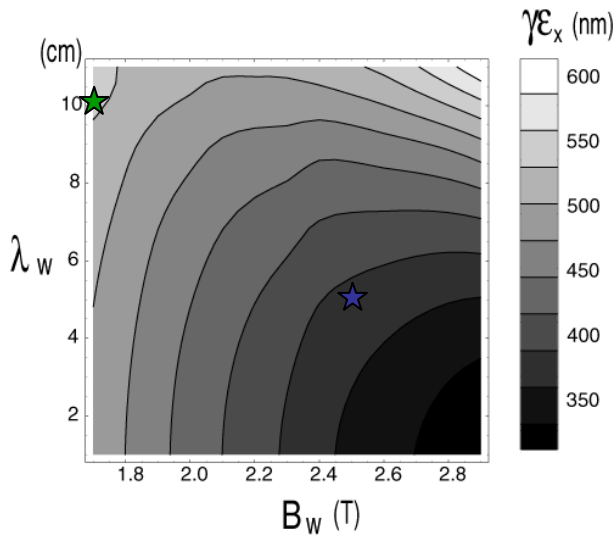

Fig. 1 Contour plot of horizontal emittance as a function of wiggler peak field B_w and period length λ_w. Since the emittance coupling ratio is kept constant at 0.63%, $\gamma\varepsilon_y$ is given by $0.0063\cdot\gamma\varepsilon_x$. The green and blue stars indicate the parameters of the PM and SC wiggler discussed in the next section.

Fig. 2 shows this optimum value as a function of λ_w together with the achieved emittance value.

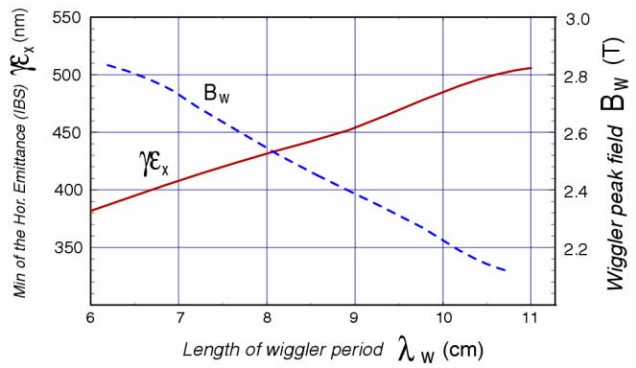

Fig. 2 Optimum wiggler field and corresponding horizontal equilibrium emittance as a function of wiggler period length.

WIGGLER TECHNOLOGY

For the damping wigglers two different types of wiggler technology are considered.

The first design is a room-temperature permanent magnet wiggler based on NdFeB material. This wiggler type uses the same design principles as the wigglers which have been developed for PETRA III [8]. A schematic of the wiggler is depicted in Fig. 3. Fig. 4 shows the distribution of magnetic flux in such a design. The wedge-shaped pole design has in comparison with more conventional permanent magnet wigglers the advantage of a reduced magnetic volume and an almost vanishing magnetic coupling between adjacent poles. The latter feature simplifies drastically the adjustment procedures for field flatness.

The second wiggler design is based on NbTi superconducting magnet technology. For this wiggler a solution is proposed where the upper and lower half of the wiggler is wound with a single-piece conductor wire each, instead of manufacturing a number of individual coils (Fig. 5). This helps reducing the period length for rather high magnetic field and avoiding many interconnections between adjacent pole coils. Two symmetrical iron yokes (upper and lower) together with a fiberglass plastic spool support the single coil (for each half) without any interconnections between the poles. The conductor wire transition (foldover) from pole to pole is performed in a groove cut in the fiberglass spool. Fig. 6 shows a preliminary design of the s.c. wiggler. The two wiggler halves are separated by stainless steel spacers in the wiggler gap.

Table 1 summarises the main parameters of both wiggler designs. As an additional design constraint a minimum full-aperture height available for the beam of 12 mm has been imposed. The values of B_w are somewhat lower than the optimum values inferred from fig. 2.

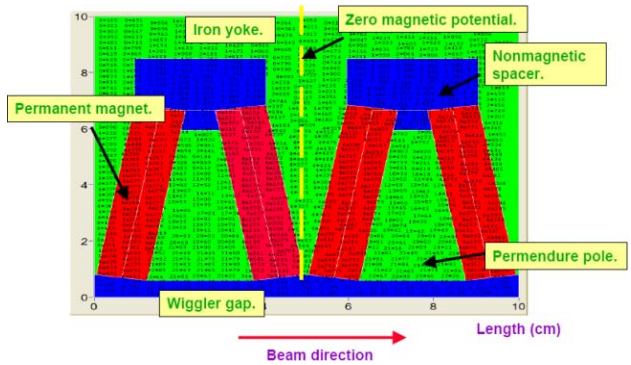

Fig. 3 Schematic view of permanent magnet wiggler design.

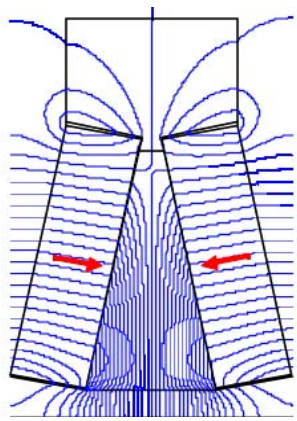

Fig. 4 Magnetic field lines for permagnet magnet wiggler design.

Table 1 Wiggler parameters

		Permanent magnet	Super conducting (NbTi)
Period length	cm	10	5
Total height of beam aperture	mm	12	12
Peak field on axis	T	1.7	2.5
Length of wiggler module	m	2	2
Transverse field flatness at +/-1cm	%	<0.1	<0.1
Operating temperature	K	Room temperature	4.2 K

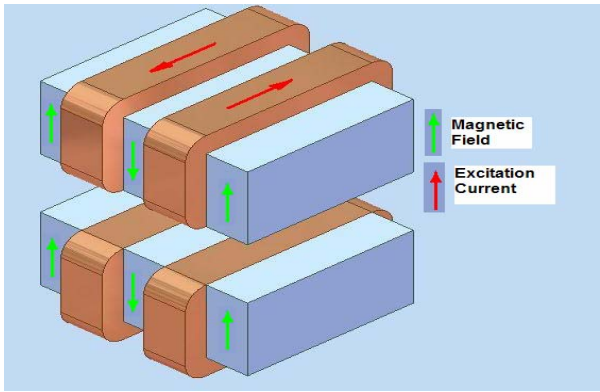

Fig. 5 Schematic view of the superconducting magnet wiggler design.

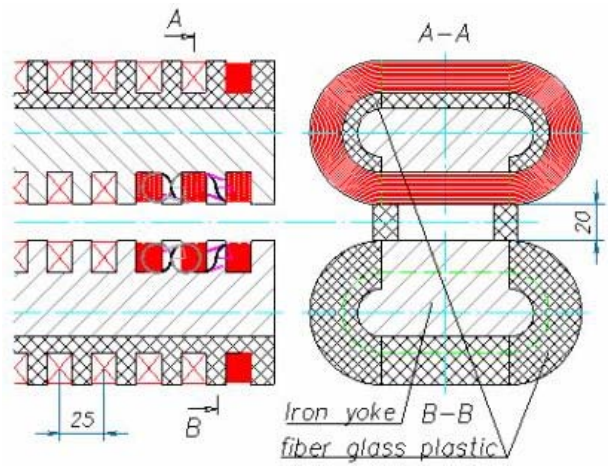

Fig. 6 Preliminary drawing of the s.c. wiggler.

Table 2 Damping ring parameters for both wiggler types

Wiggler type		PM	SC
Peak on axis field	T	1.7	2.5
Period length	cm	10	5
Beam energy	GeV	2.42	2.42
Circumference	m	364.96	364.96
Total length of wigglers	m	152	152
RF frequency	GHz	1.875	1.875
RF peak Voltage	MV	4.16	2.25
Horizontal damping time	ms	2.96	1.51
Vertical damping time	ms	2.96	1.51
Longitudinal damping time	ms	1.48	0.758
Horizontal IBS growth rate	ms	3.89	1.94
Long. IBS growth rate	ms	5.57	5.73
$\gamma\varepsilon_x$ w/o IBS	nm	131	88.5
$\gamma\varepsilon_x$ with IBS	nm	540	383
$\gamma\varepsilon_y$ with IBS	nm	3.4	2.4
emittance coupling ratio	%	0.63	0.63
ε_L with IBS	eV m	5000	5000

CONCLUSIONS AND OUTLOOK

The beam parameters resulting from the two wiggler designs are summarized in Table 2. The horizontal emittance for the superconducting wiggler design stays well below the target value of 550 nm required from the CLIC design, while the permanent magnet version just meets this goal but has no margin for effects from alignment and beam orbit errors. The damping time of the s.c. wiggler design is so fast that only a single linac pulse needs to be stored in the ring at a given time. Therefore the s.c. wiggler design is clearly favorable. We plan to build a short prototype of such a wiggler to validate the design and to determine the field quality in the beam region.

REFERENCES

[1] M. Korostelev, F. Zimmermann, “Optimization of the CLIC Damping Ring Design Parameters,” EPAC'02, Paris, 2001

[2] M. Korostelev, F. Zimmermann, “A Lattice Design for the CLIC Damping Ring,” Nanobeam'02 ICFAWorkshop, Lausanne, 2002

[3] M. Korostelev, F. Zimmermann, “CLIC Damping Ring Optics Design Studies,” PAC’05, Knoxville, 2005

[4] T. Agoh, M. Korostelev, D. Schulte, F. Zimmermann, K. Yokoya,“Collective Effects in the CLIC Damping Rings,” PAC’05, Knoxville, 2005

[5] M. Korostelev, F. Zimmermann, “Correction of vertical Dispersion and Betatron Coupling for the CLIC Damping Ring,” this conference

[6] H.H. Braun, M. Korostelev and F. Zimmermann, “Potential of Non-standard Emittance Damping Schemes for Linear Colliders,” APAC’04, Gyeongju, 2004

[7] V.S. Kuzminykh, E.B. Levichev and K.V. Zolotarev, “Evacuation of SR Power from the CLIC Damping Ring,” CLIC note 658, 2006

[8] M. Tischer, K. Balewski, W. Decking, M. Seidel, L. Yongjun, Vobly, V. Kuzminykh, K. Zolotariov, E. Levichev, “Damping Wigglers for the Petra III Light Source,” PAC’05, Knoxville, 2005